

I.N. Beckman

The application of the diffusion gas probe technique for the characterization of polymeric membrane materials.

Introduction.

New synthetic polymer, e.g. glassy polymers with microheterogeneous structure, block copolymers and polymer composite materials, containing adsorbents, catalysts, etc. have been applied recently in the technology of synthetic polymers used for preparing selective membranes [1].

Anomalies of permeability and diffusion of penetrating species in synthetic membranes encountered in experiments may have their origin in interactions between components of the penetrating agents various structure formations in hard polymeric materials. In these cases the permeability, solubility and diffusion properties of polymer membranes may strongly depend on the concentration of the penetrating species, time and the local structure properties of the polymer materials.

Obviously, for preparation of polymer membranes of required properties one should to know the mechanism of migration of the penetrating species in the materials of membranes. The mass transport mechanism of the low-weight substances can be evaluated only by using high-informative and sensibility diffusion techniques with high resolution. The techniques of diffusion probe diagnostics of polymers, such as thermodesorption spectroscopy, the method of concentration waves and autoradiography, satisfy these requirements. The main advantage of the diffusion-structural analysis technique is the possibility of reconstruction of the diffusion media spatial and energetical characteristics.

The present paper is devoted to the diffusion gas probe methods (autoradiography, thermodesorption spectroscopy and the method of concentration waves) and their application to the studies of non-homogeneous in polymer material. In the present work the mathematical, methodical, instrumental, and software supplements to all diagnostic methods mentioned above are proposed.

1. Materials.

Technically and chemically pure (recrystallized 3 times) polyethylene of high density (PEHD) with crystallinity, ϕ_c , ranging from 50 to 60% polyethelene of low density (PELD) with $\phi_c=40-50\%$ and polypropelene (PP) with isotacticity more than 99% were used for investigation. Samples in the form of $(1-2)\times 10^{-4}$ m thick films or $10\times 10\times 50\times 10^{-3}$ m blocks were prepared. PP films with large spherulite structure were prepared by prolonged (8 h) thermal crystallization in the inert atmosphere at 145°C . Polymer sample analysis in polarized light revealed that in PELD, spherulites are of diameter smaller than 5×10^{-6} m, in PEHD films, separate spherulites of $(15-20)\times 10^{-6}$ m were encountered, while the structure of PP films was represented by $(15-20)\times 10^{-6}$ m spherulites randomly distributed throughout the whole sample. Prolonged annealing of PP at 145°C led to the formation of spherulites with a diameter less than 400×10^{-6} m.

For thermodesorption spectra registration, PE with density of 0.915 and the melting point of 118°C , poly-4-methylpenten-1 (PMP-1) with density 0.820 g/sm^3 were used.

Stable gases and radioactive inert radon-222 were used as gas probes.

2. Autoradiography method (ARG)

The radioactive indicator technique, combined with autoradiography (ARG) was proposed to be applied for monitoring the diffusion process development in the solid polymer phase [2-4]. This technique is unique for visualizing sorptive nonhomogeneity of a solid matrix. In this case, the sample was first kept in the atmosphere of gas, traced by a radioactive isotope (in the mode of sorption experiment or the permeability technique). After diffusion experiment, the sample was frozen in vapor of liquid nitrogen to prevent diffusion, the radioactive gas was

removed and the sample was placed in contact with photographic plates covered by nuclear photoemulsion. After exposition, the autoradiogram was photometered on a scanning microphotometer and an array of data was obtained which characterize the distribution of the darkening density on a chosen region of the autoradiogram. The results are analyzed on computer in order to elicit the non-homogeneity of the darkening and to evaluate its size and geometrical distribution. This technique allows to determine the spectrum of the local diffusion and solution coefficients.

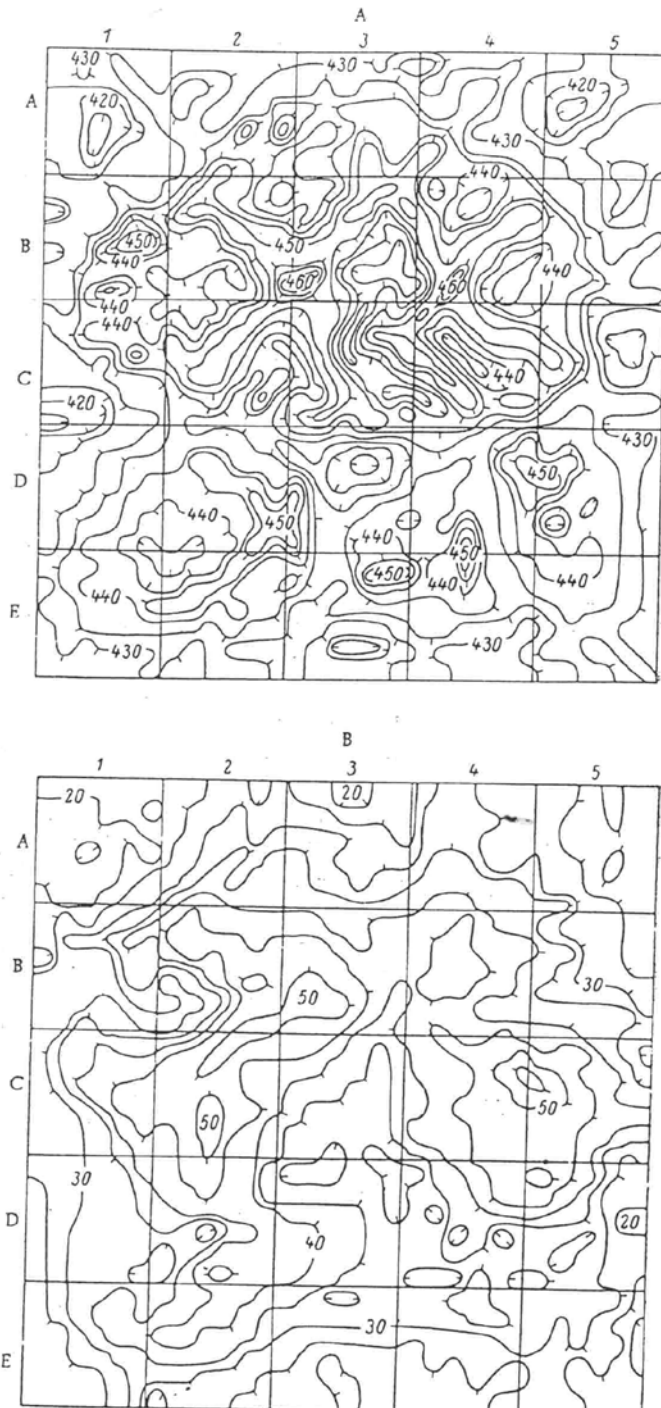


Fig. 1. Result of photometric evaluation of tr autoradiogram (radon in polypropylene with a macrospherulite structure): $t_1=160$ sec. A) entry side of the membrane; B) exit side of the membrane.

The analysis of the obtained autoradiograms showed, that diffusing radon does not decorate morphological formations in pure crystalline polymers such as PE and PP. However, in PP with large spherulite structures (diameter of spherulites reaches 2×10^{-4} m) single

accumulations in the form of "stars", made by alpha-particle tracks are detected on ARG. Comparison of ARG with photographs of PP film in polarized light revealed that accumulations are distributed along the borders of spherulites and in regions between them. Inside the spherulite, radon is in an atomically dispersed state, which is registered in the form of chaotically located tracks. At higher spherulite size (up to 5×10^{-4} m and more in diameter) radon accumulates in the form of an even layer surrounding the spherulite.

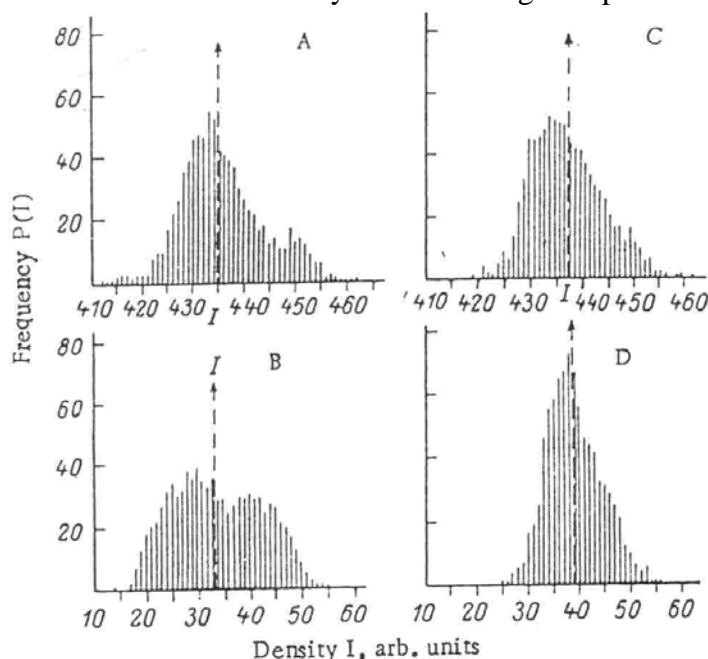


Fig. 2. Sampling of the results of photometric evaluation of the autoradiogram: A) entry side of the membrane, $t_1=160$ sec; B) exit side of the membrane, $t_1=160$ sec; C) entry side of the membrane, $t_2=220$ sec; D) exit side of the membrane, $t_2=220$ sec.

The set of the photometrical curves makes possible construction of ARG darkening density map, that characterize directly the radon distribution throughout the inlet and outlet surfaces. As an example, there are results of the photometry of the radon autoradiogram in the PP of high spherulitic structure in the mode of steady gas flow through the membrane from the inlet and outlet sides of the membrane given in Fig.1a and 1b. The data are given in form of isolines drawn through equal darkening density values. As it can be seen in the figure, the darkening density distribution is not even: there are as the large-sized regional, as the numerous local anomalies. Basing upon data in figure 1, the distribution of the darkening given values appearance frequencies upon the darkening density were calculated and presented in Fig.2a and 2b. The both darkening distribution have approximately symmetrical character and the distribution at the inlet is considerably wider then that at the outlet. For the obtained results interpretation, we introduce the term of the local solubility coefficients spectrum. Speaking about the local coefficient, we assume a coefficient evaluated for a certain separate volume element of polymer, having approximate dimensions as $(10 \times 10 \times 50 \mu\text{m})$, where $50 \mu\text{m}$ is the α -particle track length in the material). As it follows from fig.2, a certain amount of gas adsorbed on the inlet surface does not take part in the diffusion. The phenomena observed may be caused by the higher sorption capacity of some parts of the sample inlet surface. From our point of view, Fig.2b presents the true spectrum of local solubility coefficients.

Having the darkening similar to that in Fig.1 but obtained at the diffusion times lower than the time required for the steady state regime establishment we can calculate the chart of the local diffusion coefficient distribution on the membrane surface. In this particular case the local diffusion coefficient is averaged onto the surface area $(10 \times 10 \mu\text{m})$. На рисунке 3 представлена функция плотности распределения локальных коэффициентов диффузии. As it is seen in the fig.3, the spectrum has continuous character and the right-hand symmetry. It mean that there

is a small number of diffusion ways with abnormally high values of diffusion coefficients in this spectrum.

Thus, it can be concluded that the autoradiographical variant of the permeability method allows to obtain the quantitative characteristics as of the spatial distribution of the gas solubility coefficients in polymer, as of the diffusion process evaluation in space and time.

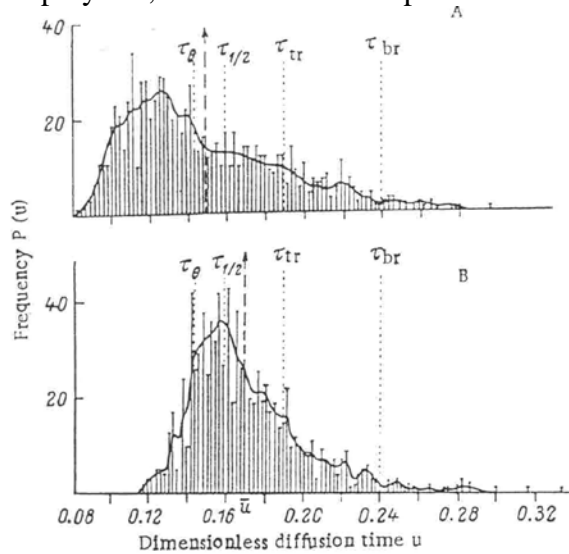


Fig. 3. Frequency distribution function for the dimensionless diffusion time: A) diffusion time $t_1=160$ sec; B) diffusion time $t_2=220$ sec.

3. Concentration waves method (CV).

The method of concentration waves is based on the passage of harmonic oscillation of penetrant concentration through a polymer sample. Being compared with the classical version of permeability method, the method of concentration waves provides additional degrees of freedom: the time of output towards the periodical steady-state condition, the equilibrium position, the amplitude and phase shift of the passed wave. An additional degree of freedom results from the possibility of performing the experiment at various frequencies. The concentration waves diminish with an increase of frequency [5].

We assume that at the membrane inlet the gas probe concentration is altering according to the following relationship:

$$C=0,5C_0(1+\sin\omega t) \quad (1)$$

where $C_0 = \sigma\rho_0$ is the gas concentration at the membrane inlet, σ is the gas solubility constant, ρ_0 is the partial gas pressure, ω is the oscillation frequency, t is the time.

In the established periodic process at the membrane outlet the probe flux will also alter according to the sin law with the same oscillation frequency ω but with another amplitude value and with the phase shift relating the initial wave:

$$J_t=A\sin(\omega t+\varphi) \quad (2)$$

where amplitude of the wave passed through the sample is:

$$A = \frac{\frac{DC_0S}{l} l \sqrt{\frac{\omega}{D}}}{2 \sqrt{\text{sh}^2 \left(l \sqrt{\frac{\omega}{2D}} \right) + \sin^2 \left(l \sqrt{\frac{\omega}{2D}} \right)}} \quad (3)$$

and the phase shift:

$$\varphi = \arcsin \left[\frac{\cos(z)\text{sh}(z) - \sin(z)\text{ch}(z)}{\sqrt{2[\text{sh}^2(z) + \sin^2(z)]}} \right] \quad (4)$$

where $z = l\sqrt{\frac{\omega}{2D}}$, D is the probe diffusion coefficient in the membrane material, S is the membrane surface square, l is the membrane thickness.

As it is known, by increasing the oscillation frequency, the passed wave amplitude $A(\omega)$ decreases (the membrane let the low-frequency oscillations pass through and it cuts out those of high-frequency) and the phase shift $\varphi(\omega)$ passes its minimum value and then is subject the periodic oscillations.

The characteristics of the concentration waves passage through the material can be conveniently interpreted in form of the amplitude-phase diagram where the amplitude value corresponds to the vector length, and Π the phase shift corresponds to the angle of наклона. The spiral width is conditioned by the diffusion coefficient (to be more exact by the permeability constant, $P = \sigma D$). If the amplitude-phase diagram is presented in the normalized form (i.e. in form of A/A_0 , where A is the amplitude of the passed wave, and A_0 is that of the initial one), then in case of an "ideal" Fick's diffusion in a homogeneous media the obtained curve does not depend upon the parameters of the gas transport in membrane (Curve 1 from Fig.4).

Another way of the CV results interpretation is the Lissageou figures construction, where the passed wave amplitude is fixed on the ordinate axis, and the initial wave amplitude is fixed on the abscises axis. In the case of homogeneous media (i.e. classic diffusion mechanism) Lissageou figure has linear shape that passes the origin and makes 45° angle with the abscises axis. At the classic diffusion mechanism the Lissageou figure does not depend upon the oscillation frequency.

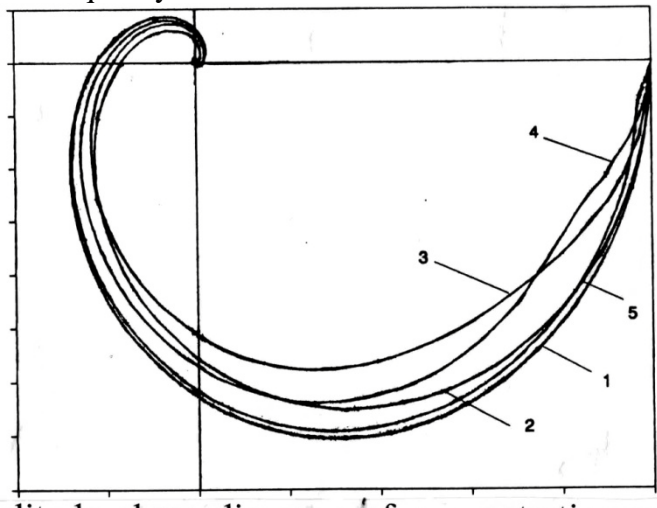


Fig.4 The amplitude-phase diagrams of concentration waves passed homogeneous media with two independent diffusion paths. Curves: 1 – homogeneous media; 2 – parallel diffusion ($D_1=1 \times 10^{-5}$ cm²/sec; $D_2=2 \times 10^{-5}$ cm²/sec); 3 – parallel diffusion ($D_1=1 \times 10^{-5}$ cm²/sec; $D_2=5 \times 10^{-5}$ cm²/sec); 4 – parallel diffusion ($D_1=1 \times 10^{-5}$ cm²/sec; $D_2=1 \times 10^{-4}$ cm²/sec); 5 – parallel diffusion ($D_1=1 \times 10^{-5}$ cm²/sec; $D_2=5 \times 10^{-4}$ cm²/sec).

Now let us consider the concentration waves passage through nonhomogeneous media. We analyze the case of parallel diffusion in two-component media, i.e. we assume that the probe diffusion occurs by two independent ways. Let the first diffusion way be characterized by a diffusion coefficient D_1 , solubility constant σ_1 and its contribution $\phi_1=S_1/S$, and the second - D_2 , σ_2 and $\phi_2=S_2/S$ ($S_1+S_2=S$, $\phi_1+\phi_2=1$). If the gas concentration at the membrane inlet is described by eq.1, then the flux at the outlet will be again described by the eq.2, where the amplitude is expressed as follows:

$$A_B = A_1 \sin(\omega t + \varphi_1) + A_2 \sin(\omega t + \varphi_2) = A_{12} \sin(\omega t + \varphi_{12}) \quad (5)$$

where

$$A_{12}^2 = A_1^2 + A_2^2 + 2A_1A_2 \sin(\varphi_2 - \varphi_1) \quad (6)$$

$$\varphi_{12} = \arctg \left[\frac{A_1 \sin \varphi_1 + A_2 \sin \varphi_2}{A_1 \cos \varphi_1 + A_2 \cos \varphi_2} \right] \quad (7)$$

and A_1, A_2 are defined by eq.3 by substitution of $D; C_0; S$ for $D_i; C_{10}; S_i$, and φ_1, φ_2 are defined by eq. (4).

When the parallel diffusion mechanism by two independent ways is realized in the membrane, the form of Lissageou figures essentially differs from that one in case of homogeneous media. As an example, the Lissageou figures for the case when $D_1=2 \cdot 10^{-5}$ cm^2/sec , $D_2= 1 \cdot 10^{-5}$ cm^2/sec ; $\sigma_1=\sigma_2$; $S_1=S_2$; ($\phi_1=\phi_2=0.5$) are given in fig.5. It is evident that the figures become elliptical and the absolute values of the major and the minor ellipse axes, their ratio and the orientation of the major ellipse axis relatively the abscissa axis depend upon the oscillation frequency: as the oscillation frequency ω augments, the ellipse compresses and rotates.

The existance of two independent diffusion paths in the sample makes influence upon the form of the amplitude - phase diagram (curves 2-5 from Fig. 4). As it is clear from the figure, at low frequencies the curve 2 (parallel diffusion) coincides with the curve 1 (classical diffusion), the mass-transfer occurs by the both diffusion paths. As the frequency increases the curves 1 and 2 start to deviate (interference of the waves occurring by the both paths). At higher frequencies curves 1 and 2 coincide again (the wave passes through one path that makes the most contribution into the total flux, and the second path becomes "invisible". Obviously, there is a certain range of oscillation frequencies $\omega_0 \leq \omega \leq \omega_r$ where the amplitude-phase diagram is sensible to the structural nonhomogeneities. There are no other frequency values beyond that interval where the presence of more than 1 diffusion path could be observed.

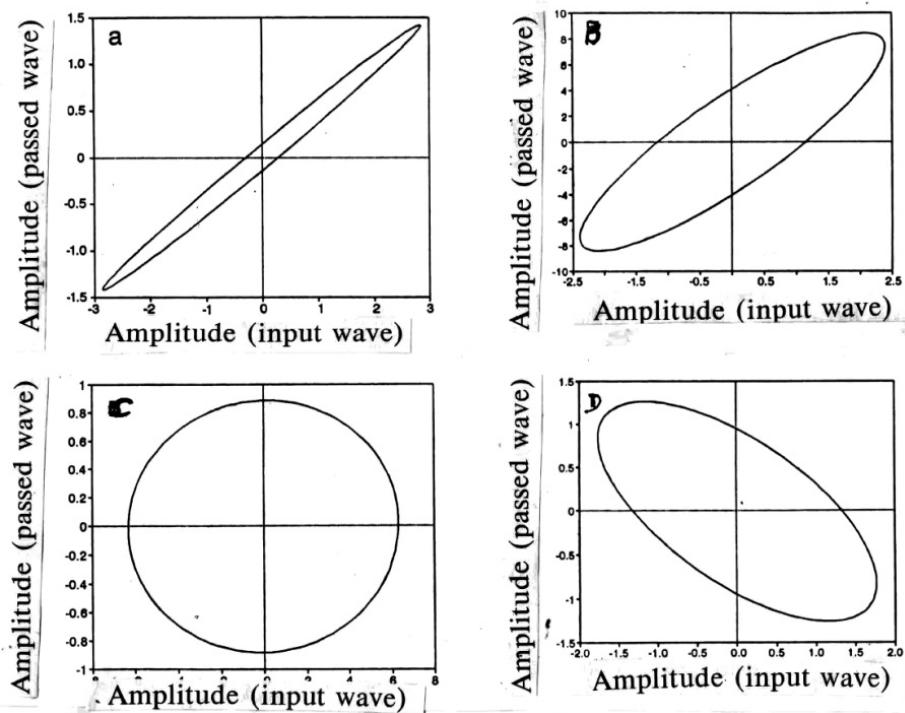


Fig.5 Dependence of Lissageou figures upon oscillation frequency of concentration waves passed media with two independent diffusion paths: $D_1=1 \cdot 10^{-5}$ cm^2/sec ; $D_2=2 \cdot 10^{-5}$ sm^2/sec . Curves: frequency 0,01 (a); 0,1 (b), 0,5 (c); 1 (d) sec^{-1} .

Therefore, the concentration waves method makes possible to reveal structural non-homogenities in the sample that influence the mass-transfer processes. This method can be applied, for example, for the microfissures identification that arise in the selective membrane in course of its continuous functioning in the mode of gas separation. The criterion of the parallel diffusion mechanism realization in the material is the dependence of the Lissageou figures form and the normalized curves of the amplitude-phase characteristics upon the oscillation frequency.

CV method allows to distinguish the diffusion media with layers orientated in parallel with the mass flux from the media with randomly distributed point defects.

4. Thermodesorption spectroscopy method (TDS).

The thermodesorption spectroscopy method is based upon gas insertion into a polymer under special conditions and the consequent study of gas release kinetics in the regime of the programmed heating, linear as a rule. The curves of the sample weight loss or the released gas flux dependence upon time or temperature are registered in the course of the experiments. From the dependencies obtained, the spectrum of energetic states of the diffusant is evaluated. By applying the TDS method, an experimental parameter alteration can be performed: the diffusant partial pressure at its insertion into the sample, the time and temperature of diffusion annealing and preliminary outgassing, the type of the gas used and the rate and regime of heating. By means of varying those parameters, the gas can be inserted into a definite morphological form of the material, and the energy spectrum of the diffusant molecules in the polymer can be varied in a wide range [6,7].

As an example, we shall consider the curves of thermostimulated release of radon from PELD and PMP-1. Radon was inserted by diffusion from the gaseous phase at given temperature. Then the sample was frozen in liquid nitrogen and placed into the device for studies of the gas release under thermal influence [8]. In course of the experiment in the linear heating regime the dependence of the gas flux released from the sample upon temperature (time) was registered. The installation allowed to perform the heating from the temperature of the liquid nitrogen (from -196°C upto 400°C) with the heating rate of $3\text{-}15^{\circ}\text{C}/\text{min}$. Alteration of time and/or temperature and time of the subsequent preliminary degassing allowed to vary the initial gas distribution in the polymer sample.

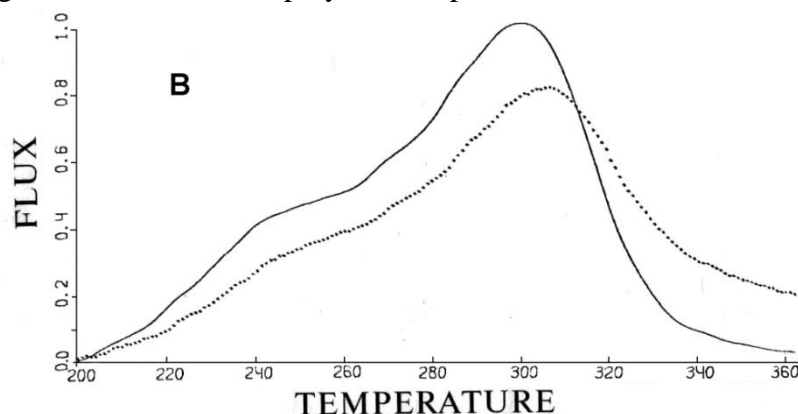


Fig.6 The typical curve of radon release from poly-methylpentene-1 in the regime of the linear heating.

The typical TDS curve of radon release from PELD is given in Fig.6a. The curve has a form of a single peak, the temperature of its maximum point is $20\text{-}70^{\circ}\text{C}$ and depends upon the sample thickness and the heating rate. A software package that provides processing of experimental TD spectra in terms of different diffusion mechanisms has been worked out by the authors of the present work [9]. It; was found that the form of experimental TD spectra is well described within the bounds of so called kinetic regime of degassing. The formal power of gas release kinetics was found to be 1.1 ± 0.2 . The effective activation energy is 12 ± 2 ккал/моль.

TD spectrum of radon from PMP-1 is given in Fig. 6b. The gas release process starts at low temperatures (200 K). There are two peaks of gas release in the curve, one of them in the region of $240\text{-}260$ K that is apparently connected with the solid state phase transition that occurs in PMP-1 in that temperature interval. The activation energy of gas release for this peak is 5.6 ± 0.4 kcal/mol. Another peak was found at temperature of 300 K. The activation energy that corresponds this peak was found to be 9.8 ± 0.6 kcal/mol that is in accordance with the one determined by independent experiments on radon permeability through that polymer.

List of publication.

1. D.R.Paul, Y.P.Yampol'skii (Eds.), Polymeric gas separation membranes, Boca Raton, CRC Press, 1994, 23 p,
2. I.N. Beckman, I.M.Buntseva, State of radon in crystalline polymers, Radioanal.Nucl. Chem., Letters 153 (1991) 345-355.
3. I.N. Beckman, Experimental methods of study of radioactive gases diffusion in solids. 3. Autoradiographic variant of permeability method, Radiochimia, 23, 760-766.
4. I.N. Beckman, A.A.Shviryayev, Experimental methods of study of radioactive gases diffusion in solids. 6. Topological features of diffusion processes, Radiochimia, 24 (1982), 126-135.
5. I.N. Beckman, A.B.Shelekhin, Separation of gas mixtures in unsteady-state conditions, J. Membrane Sci., 55 (1991) 283-297.
6. A.V.Zheleznov , I.N.Beckman, V.Balek, Theory of emanation thermal analysis. 7. Thermostimulated inert gas release as influenced by the energy spectrum of the defect sites in solids, Thermochim. Acta, 142 (1989), 251-264.
7. A.V.Zheleznov , I.N.Beckman, V.Balek, Theory of emanation thermal analysis. 8. Influence of sample-labelling conditions on the thermostimulated inert gas release.- Thermochim. Acta, 143 (1989) 27-35.
8. I.N. Beckman, Experimental methods of study of radioactive gases diffusion in solids. 9. Equipment and technique of radioactive gas probe method, Radiochimia, 29 (1987), 542-549.
9. I.N.Beckman, A.V.Zheleznov, V.Balek, Evaluation of thermal analysis experimental data. I. Computer modelling and interpretation of thermal decomposition of solids studied by evolved gas analysis and thermogravimetry, J. of Thermal Analysis, 37 (1991) 1479-1495.